

UNCLASSIFIED

SECURITY CLASSIFICATION OF THIS PAGE

(2)

REPORT DOCUMENTATION PAGE

Form Approved
OMB No. 0704-0188

1a. REPORT SECURITY CLASSIFICATION

UNCLASSIFIED

2a. SECURITY CLASSIFICATION AUTHORITY

AUG 18 1989

DATE

BER(S)

B

1b. RESTRICTIVE MARKINGS

THE FILE COPY

3. DISTRIBUTION/AVAILABILITY OF REPORT

APPROVED FOR PUBLIC RELEASE
DISTRIBUTION IS UNLIMITED

5. MONITORING ORGANIZATION REPORT NUMBER(S)

AFOSR-TR-89-1136

AD-A211 944

6b. OFFICE SYMBOL
(if applicable)

7a. NAME OF MONITORING ORGANIZATION

AFOSR/NA

STANFORD UNIVERSITY

6c. ADDRESS (City, State, and ZIP Code)

AERONAUTICS DEPT
STANFORD, CA 94305

7b. ADDRESS (City, State, and ZIP Code)

BUILDING 410
BOLLING AFB, DC 20332-64488a. NAME OF FUNDING/SPONSORING
ORGANIZATION

AFOSR

8b. OFFICE SYMBOL
(if applicable)

NA

9. PROCUREMENT INSTRUMENT IDENTIFICATION NUMBER

AFOSR 84-0099

8c. ADDRESS (City, State, and ZIP Code)

BUILDING 410
BOLLING AFB, DC 20332-6448

10. SOURCE OF FUNDING NUMBERS

PROGRAM
ELEMENT NO.

61102F

PROJECT
NO.

2307

TASK
NO.

A3

WORK UNIT
ACCESSION NO.

11. TITLE (Include Security Classification)

(U) UNSTEADY AERODYNAMICS WITH APPLICATIONS TO FLIGHT MECHANICS

12. PERSONAL AUTHOR(S)

ASHLEY

13a. TYPE OF REPORT

FINAL

13b. TIME COVERED

FROM

LAPRS 4-31-3-89

14. DATE OF REPORT (Year, Month, Day)

06/89

15. PAGE COUNT

10

16. SUPPLEMENTARY NOTATION

17. COSATI CODES

FIELD GROUP SUB-GROUP

18. SUBJECT TERMS (Continue on reverse if necessary and identify by block number)

UNSTEADY AERODYNAMICS, DELTA WING FLOWS

19. ABSTRACT (Continue on reverse if necessary and identify by block number)

Unsteady airload measurements have been made on a series of low aspect ratio delta wings subjected to transient pitch motions. These data have been qualified and discussed in several publication which are listed. In addition a discussion on the relevance of unsteady transient airloads to flight mechanics is included.

20. DISTRIBUTION/AVAILABILITY OF ABSTRACT

☐ UNCLASSIFIED/UNLIMITED ☒ SAME AS RPT. ☐ DTIC USERS

21. ABSTRACT SECURITY CLASSIFICATION

UNCLASSIFIED

22a. NAME OF RESPONSIBLE INDIVIDUAL

HENRY E. HELIN

CAPT USAF

22b. TELEPHONE (Include Area Code)

202-767-0471

22c. OFFICE SYMBOL

AFOSR/NA

STANFORD UNIVERSITY
Department of Aeronautics and Astronautics
William F. Durand Building
Stanford, California 94305

June 1989

To: Capt. H. E. Helin, Ph. D.
Program Manager, Fluid Mechanics
AFOSR/NA
Building 410, Room A223
Bolling Air Force Base
Washington, DC 20332-6448

AFOSR-TR. 89-1136

From: Holt Ashley, Principal Investigator

Subject: Grant AFOSR 84-0099 - Final Scientific Report

Publication and Related Matters

For the four years of Stanford's research activity under this grant, it is believed that the most significant "products" are the substantial number of publications and the advanced graduate students whose theses formed the foundations of those publications. Nearly all of these students, along with a host of others whose work was supported by OSR over a continuous period beginning in 1953, are now constructively employed in academia, industry or the laboratories of allied governments around the world. Their names are recorded as authors or coauthors of archival papers, SUDAAR reports, reports of the MIT Aeroelastic & Structure Research Laboratory, etc.

At the beginning of the attached list of references, the Principal Investigator has attempted, in roughly chronological order, to summarize most of the papers whose contents were wholly or partially supported by the grant. Some of these have been published, in whole or part, by archive journals subsequent to issuance of the cited report; others will be in the near future.

Many opportunities have occurred, and will continue to occur, for less formal communication of recent research discoveries. Several of these have already been described to OSR, for example in the rejected proposal Aero No. 1-89 submitted in Sept. 1988 and in the annual Interim Scientific Reports. As part of the process of completing his doctoral requirements, candidate M. Ameen Jarrah summarized his experimental program at a Stanford Fluid Mechanics Seminar in December 1988. By invitation, the Principal Investigator gave talks on the unsteady flow, agile-aircraft maneuvers and loads findings to engineers of Boeing Commercial Airplanes on March 28, 1989, to Boeing Military Airplanes in Wichita on June 28, 1989, and to a seminar audience at San Diego State University on March 8, 1989.

As a final observation, it is noted that aerospace organizations around the world have not all lost sight of the Principal Investigator's career of contributions to research and teaching in unsteady aerodynamics, aeroelasticity and related fields. In October, 1987, he was awarded the Ludwig Prandtl Ring by DGLR, the West Germany aerospace professional society (one of a total of five such recognitions for living Americans). In December, 1988, the British Royal Aeronautical Society selected him as one of its two Honorary Fellows for that year. In June, 1989, the West German research institution DLR invited him to give the keynote after-dinner speech on applied optimization for their Seminar on Optimization in Bonn; this was one of their annual series of high-level technical seminars on chosen topics in the field.

Summary of Research Prior to Mid-1988

This activity has been fully described in three of the aforementioned Interim Scientific Reports, dated in April or early May of 1986, 1987 and 1988. By way of summary and prior to the work of Dr. Jarrah described in more detail below, it is believed that the principal contributions supported by the grant are those extensively reported in the dissertations of Dr. van Niekerk (published in Refs. I and II), Dr. Brandao (Ref. VI) and Dr. Azevedo (Ref. VII). It should be mentioned that the last two individuals were Brazilian nationals and that, in considerable part, their work and attendance at Stanford were funded by that government. Especially in the case of Dr. Azevedo, however, there was substantial involvement of the grant; this is being recognized in the resulting publications in the usual way.

Azevedo's accomplishments are regarded as particularly outstanding and of substantial interest to U. S. Air Force, with the impending payload launches by the Titan IV series of booster configurations. Starting from first principles but some 25 years after the incidents which he analyzed, he was able to predict successfully an instability of "hammerhead" payloads on ballistic launch vehicles. In so doing he coupled a linear-elastic representation of the LV, based on superposition of its first three natural modes of free-free bending vibration, with a transonic, unsteady CFD code employing approximate Navier-Stokes equations with a modified Baldwin-Lomax relation between shear stresses and rates of strain. The latter was adapted from axisymmetric, steady-flow codes developed by Pulliam. For an Atlas-Able vehicle which encountered difficulty of this kind in the early 1960's, he predicted a high-q, transonic instability of what aeroelasticians call the "single-degree-of-freedom" variety for the 17-Hz second mode. The first and third modes were found to be quite stable, a prediction which agreed with in-flight observation as well as could be ascertained.

Summary of Recent Research in 1988 and 1989

The bulk of this report deals with progress, prior to and during the cited period, on Dr. Jarrah's unsteady high-angle-of-attack testing and preliminary attempts to make applications of his results. The experimental effort relied completely in the availability of time in one of the 7' x 10' low-speed wind tunnels at NASA Ames Research Center. In this connection the project was indebted since early 1987 to Mr. Richard Margason, Chief, Fixed-Wing Aerodynamics Branch, as well as to Mr. Tim Naumowicz, who is an engineer assigned to that branch. They arranged for tests to take place during two extended periods, the first in late August and September, 1987, and the second in April and May of 1988. NASA also furnished the strain-gauge balance, laser illumination, large quantities of hardware and software for data handling, and personnel support before and during the tunnel entries. The dollar value of this support is estimated at well over \$10,000.

In November, 1987, Mr. Margason suggested that particular measurements of interest to NASA might be included in the program through a joint research interchange with Stanford under what is called the NASA Ames University Consortium. The conversations resulted in the award of Contract NCA2-287, entitled "Unsteady Flow Measurements on Delta Wing Models Forced to High Angles of Attack." With Margason and the Principal Investigator as collaborators, this was for a period of one year commencing January 1, 1988, and funded at \$25,000. The collaboration was entirely complementary to the activity supported by OSR, and the Project Monitor was notified in a timely fashion. More detail is given about this arrangement in the 1988 Interim Scientific Report. The intention, if Dr. Jarrah is able to complete plans to visit Stanford during the summer of 1989, is that a final report on the NASA contract will be issued in the form of a Technical Note presenting all of the data obtained under the program.

The OSR-supported investigation during this recent period is believed to be so well described in the last paper prepared by Dr. Jarrah and the Principal Investigator (Ref. X) that an Appendix is attached hereto adapted from that document. Any question about those results or other accomplishments under the grant can be directed to the Principal Investigator, telephone (415) 723 4136.

Ev.	
Distribution/	
Availability Codes	
Dist	Avail and/or Special
A-1	

LIST OF REFERENCES

- I. van Niekerk, B., "Computation of Second-order Accurate Unsteady Aerodynamic Generalized Forces," AIAA Journal, Vol. 24, No. 3, March 1986, pp. 492-498.
- II. van Niekerk, B. "Integration of Singular Functions Associated with Lifting Surface Theory," AIAA Journal, Vol. 24, No. 7, July 1986, pp. 1194-1195.
- III. Ashley, H., "On the Feasibility of Low-speed Aircraft Maneuvers Involving Extreme Angles of Attack," Journal of Fluids and Structures, Vol. 1, No. 3, July 1987, pp. 319-335.
- IV. Ashley, H., and Clarke, L., "On the Feasibility of Low-speed Fighter Maneuvers Involving Extreme Angles of Attack," SUDAAR 563, Department of Aeronautics and Astronautics, Stanford University, July 1987.
- V. Lee, I., "Resonance Prediction for Slotted Wind Tunnel by the Finite Element Method," No. 86-0898, AIAA et al. 27th Structures, Structural Dynamics and Materials Conference, May 1986, San Antonio, TX, pp. 256-265 (published in AIAA Journal).
- VI. Brandao, M. P., "On the Aeroacoustics, Aerodynamics and Aeroelasticity of Lifting Surfaces," SUDAAR 565, Department of Aeronautics and Astronautics, Stanford University, Feb. 1988.
- VII. Azevedo, J. L. F., "Transonic Aeroelastic Analysis of Launch Vehicle Configurations," Ph. D. Dissertation, Department of Aeronautics and Astronautics, Stanford University, Feb. 1988 (issued as NASA CR 4186, Oct. 1988).
- VIII. Naumowicz, T., Jarrah, M. A., and Margason, R. J., "Aerodynamic Investigation of Delta Wings with Large Pitch Amplitude," AIAA 88-4332-CP, presented at AIAA Atmospheric Flight Mechanics Conf., Minneapolis, MN, August 1988.
- IX. Jarrah, M. A., "Low-speed Wind-tunnel Investigation of the Flow about Delta Wings, Oscillating in Pitch to Very High Angle of Attack," AIAA 89-0295, presented at 27th Aerospace Sciences Meeting," Reno, NV, January 1989.
- X. Jarrah, M. A., and Ashley, H., "Impact of Flow Unsteadiness on Maneuvers and Loads of Agile Aircraft," AIAA 89-1282, presented at AIAA/ASME/ASCE/AHS/ASC 30th Structures, Structural Dynamics and Materials Conference, Mobile, AL, April 1989 (submitted for publication to Journal of Aircraft).

APPENDIX

IMPACT OF FLOW UNSTEADINESS ON MANEUVERS AND LOADS OF AGILE AIRCRAFT

M. Ameen Jarrah*
and
Holt Ashley**

Department of Aeronautics and Astronautics
Stanford University, Stanford, California 94305

Abstract

The paper begins by reviewing a new program of unsteady airload measurements executed on a family of low-aspect-ratio delta wings and motivated by recent interest in "supermaneuvers" as a capability of the next generation of aircraft designed for air-superiority missions. In transient pitch motions for time constants and maximum α 's which reproduce full-scale, normal force and other loads significantly exceed steady-state values when x is increasing but fall far below on the downstroke. For a series of examples involving "generic" supermaneuvers taken from the literature, implications of this discovery are illustrated. Turn rates are achieved which can be considerably greater than what one would predict with steady wind-tunnel data. This increase in agility does not, however, necessarily require a penalty in terms of increased structural loads. A simplified "theory" is proposed, trying to show how the important influence of the leading-edge vortex instability might empirically be incorporated into loading estimates for wings with sharpened edges. Conclusions are stated regarding the introduction of these findings into the design of such aircraft.

Nomenclature

AR $(=b/S)$ Wing aspect ratio
b Wing span
c Wing chord
 \bar{c} Mean aerodynamic chord
 $C_D, C_L, C_m, C_n, C_{\dot{m}}$ Coefficients of drag, lift, pitching moment, normal force and rolling moment (standard aeronautical definitions)
 C_{D0} Drag coefficient of plate normal to airflow
 C_{m0} Pitching moment about model axis
D Drag force
g Acceleration of gravity

*Research Assistant; Ph.D. awarded January 1989. Student member, AIAA

**Professor. Honorary Fellow. AIAA.

h Altitude
k $(=\Omega c_0/2V)$ Reduced frequency
K $(=\dot{\alpha}_{max} c_0/2V)$ Pitch-rate parameter
L Lift force
m Mass of flight vehicle
 M_x Pitching moment about pitch axis
 n_x Normal load factor
N Normal force on wing
q $(=\rho V^2/2)$ Flight dynamic pressure
 Ω Angular velocity in pitch
Re Reynolds no. based on midspan chord
S Plan area of wing
t time
T Thrust force
V speed of flow or flight
x, y, z Cartesian coordinates (x measured aft from vertex of delta wing)
 $x_b(t)$ x-coordinate for vortex breakdown
 x_{00} x-coordinate of pitch axis
X Azimuth angle of flight path

Greek letters

α Angle of attack
 β Angle of sideslip
 Γ Flight-path angle above horizontal
 Ω Sweep angle of wing leading edge
 ρ density of air
 ϕ Bank angle about velocity vector
 Ω Circular frequency of sinusoid

Subscripts, etc.

(\cdot) Time derivative
(\cdot)₀ Cartesian coordinates in horizontal plane
(\cdot)_{max} Maximum value of time function
(\cdot)₀ Reference value (c_0 is midspan chord of wing)

Introduction

The tactical advantages of "supermaneuvers" in short-range combat between air-superiority aircraft were first pointed out in the open literature by Herbst (Refs. 1, 2 and several more recent publications). They are effective at very low speeds, where transients of angle of attack α to 50° and above can be performed without exceeding acceleration-tolerances of

aircrew or structure. They have also motivated a great deal of research in vehicle dynamics, trajectory optimization, aerodynamics and related fields. Important studies of optimized supermaneuvers by Well, Faber and Berger⁽²⁾ appeared in the early 1980's. The many collections of papers on the topic are typified by AGARD Conferences (e.g., Dietz and Duc⁽³⁾) and the USAF Technical Specialists Meeting⁽⁴⁾.

It is noteworthy that published analyses of high- α tactics have, for lack of better information, been forced to rely on steady-state airload data. Good current examples would be presentations (e.g., Anderson⁽⁵⁾) and a panel discussion at the 1989 Aerospace Sciences Meeting. Similarly, the minimum-time turns calculated in Refs. 3 treat the fighter as a point mass, employ α and bank angle ϕ as the primary "controls," and employ steady curves for the coefficients C_L and C_D . Projected on a vertical plane, Fig. 1 reproduces an extreme case taken from that report. The vehicle starts and ends at the same point in space, except that its velocity vector & longitudinal axis are exactly reversed. The 14% time advantage thus achieved over a standard horizontal turn, with the same initial and final conditions but constrained α , can probably be increased by the clever use of some unsteady effects examined in what follows. Incidentally, one of the present authors published a rotational-dynamics study of the Ref. 3 maneuvers, in which it was shown that the required aerodynamic moment control is feasible when augmented by roughly $\pm 10^\circ$ thrust-vector control for the engine(s).

In a timely review of the needs and possibilities relevant to the design of so-called "agile" aircraft, Lang and Francis⁽⁶⁾ called attention to likely significance of flow unsteadiness for enhancing supermaneuvers (see Figs. 6, 7 and 8 of Ref. 8). The present paper undertakes to respond to their call by reexamining cases from Refs. 3 in the light of accurate unsteady measurements that have just begun to appear. It begins by summarizing some of the recent flow-visualization tests and aerodynamic data that are now available. Emphasis is placed on those tests wherein transients were performed with time constants and ranges of α which closely reproduce the maneuvers in question. The most suitable source is believed to be a program conducted by one of the present authors and partially described in Refs. 9 and 10. Next typical examples from Refs. 3 are recalculated in a simplified way that permits the significance of unsteady effects to be assessed. Finally, and in a qualitative effort to explain the root causes of time lags which occur in the airloads, results of an empirical "theory" are compared with lift and pitching moment data for a delta wing of AR = 1.

Unsteady Aerodynamics of Low-AR Wings

With regard to the steady flow patterns and airloads experienced by low-AR surfaces or complete aircraft, exposed to low-speed water or airflow but moderate to very high α , the literature is extensive. One can cite general surveys such as Refs. 11-13 and the forthcoming book by Rom⁽¹⁴⁾. Each contains useful theoretical and experimental information with an emphasis on delta planforms, either isolated or in combination with simple bodies. The key features of these flows are, of course, the pattern of separated vortices which exists above the lee surfaces and the manner in which increasing α produces progressive development of instabilities. Visualization by the illumination of smoke traces, etc., has contributed a great deal to their understanding. A seminal, definitive example was presented by Lowson⁽¹⁵⁾ this year.

Qualitative work on the consequences of time-dependent wing motion seems to have begun in Great Britain during the early 1960's. Thus a recent investigation by Thompson, Batill & Nelson⁽¹⁶⁾ cites Lowson's 1964 discovery⁽¹⁷⁾ of a hysteresis loop in the location of L.-E. vortex breakdown or "bursting" above a pitching delta model with sweep $\Omega = 80^\circ$. When it is a question of motions which begin to reproduce the α -variations anticipated for supermaneuvers, however, sources known to the authors are limited in both numbers and scope. Flow visualization data, focussed on the behavior of vortex breakdown during pitch transients with various ranges of α , are given by Nelson and coauthors^(16,18), Gad-el-Hak & Ho^(19,20), Reynolds & Abtahi⁽²¹⁾, Atta & Rockwell⁽²²⁾ and Wolfelt⁽²³⁾.

Carrying out their experiments on a delta of $\Omega = 70^\circ$ and a wing-body Soltani, Bragg and Brandon⁽²⁴⁾ present force and moment coefficients for simple-harmonic pitching between $\alpha = 0^\circ$ and 55° . Their data are noteworthy in that three finite values of sideslip angle β are included, as are unusually high values of Reynolds no. Several values of reduced frequency k — over the range of really practical interest — are also attained with the wing alone. The other major past program involving airload measurements has evidently not yet received full publication but certainly deserves citation. In the Netherlands a large double-delta model with Ω 's 76° inboard and 40° outboard was pitched about several mean α 's and at amplitudes up to $\pm 16^\circ$. Some data on time-dependent surface pressures, normal force and pitching moment are given by den Boer and Cunningham⁽²⁵⁾; again the Re's are high, ranging from 1.6 to 4.3 million.

As tools for examining influences of flow unsteadiness on high- α maneuvers the obvious choice must be the airload measurements reported *in extenso* by Jarrah⁽²⁴⁾, from which a small selection has already appeared in Refs. 9 and 10. Six components of force and moment were taken by strain-gauge balance from sharp-edged delta models of AR's 1, 1.5 and 2 in the #1 7 ft-by-10 ft low-speed wind tunnel at NASA Ames Research Ctr. In these tests Aluminum wings mounted on a U-shaped support were pitched by means of hydraulic actuation about an axis at two-thirds midspan chord. The angle α was varied between 0° and values up to 90°, either in a ramp-like fashion or according to the sinusoid

$$\alpha(t) = (\alpha_{\max}/2)[1 - \cos \Omega t] \quad (1)$$

Figure 2 is a schematic of the apparatus used for support and actuation. Figure 3 provides sketches of the models, including a second of AR=1 which was used for flow-visualization tests to be mentioned below. The reader is referred to Ref. 26 for extensive details on procedure, data reduction, error estimation, etc. It is added that only four of the six airload components can be reported, because side force and yawing moment were always zero within the accuracy of measurement. The angle β was held to zero in accordance with the requirements of Refs. 1-3, this being the constraint used to prevent departure into spins.

Model dimensions are given in mm by Fig. 3. Reynolds nos. based on midspan chord c_m ranged from 4.5 to 8.5 $\times 10^5$. The dimensionless parameter characterizing unsteadiness for both sinusoids and ramp motions is chosen to be

$$K = \dot{\alpha}_{\max} c_m / 2V \quad (2)$$

with V the airspeed and the time derivative of α taken at $\Omega t = \pi/2$ when Eq. (1) applies. In this case K is readily converted to the more conventional reduced frequency k ; multiplication would be by $2/\pi$ when $\alpha_{\max} = 90^\circ$. Values of K from 0 (steady flow) up to 0.08 were obtained in the wind tunnel. This may be compared with a maximum of about $K = 0.1$ for the maneuvers analyzed in Refs. 3, where in most cases the parameter was less than 0.05.

The new data are shown in Ref. 26 to correlate quite satisfactorily with steady-flow counterparts over the ranges of α , Re and AR where the latter prove to be available. Comparisons are also made, where possible, with airloads from Refs. 23, 24 and 25; again, systematic and unexplained discrepancies are not found. Figures 5 & 6 typify the present steady-flow aerodynamic coefficients. As in other examples which follow, plots y/α are shown as continuous curves since

the data-reduction system stored information at intervals of less than one degree. One exception is Fig. 6, wherein lift measurements appear as squares for the $AR=1.5$ model and are compared with two other experimental sources^{(27),(28)} and with the theory of Polhamus⁽²⁹⁾. The wing of $AR=2$ is selected for most of the illustrations here because this is the one later used in maneuver analyses. All plotted coefficients are defined according to standard aeronautical practice. For example, lift, pitching moment and rolling moment are, respectively,

$$C_L = L/(\sigma/2)V^2 S, \quad C_M = M/(\sigma/2)V^2 c_m S,$$

$$C_R = R/(\sigma/2)V^2 b S \quad (3a,b,c)$$

Moment R acts about the midspan axis. Pitching moment M is positive nose-up about the 77%-chord axis, so as to ensure that the values remain generally positive, but the reader is reminded that the pitch axis is at two-thirds the midspan chord for unsteady testing.

For the $AR=2$ delta, Figs. 6 through 9 show the histories of five aerodynamic coefficients as α is varied sinusoidally through one cycle from 0° to 90° and return. Arrows on the curves give the direction of motion. The pitch-rate parameter K -- taken as the measure of flow unsteadiness -- increases from 0.01 up to the intermediate value 0.04 when one goes through these four figures.

From careful study, a number of obvious conclusions can be drawn, nearly all of which apply for three models and for both the sinusoidal and ramp tests that went well past maximum lift. Even at values of K below 0.01 lift, normal force and drag significantly exceed the corresponding steady values at α 's above 20-25° when this angle is increasing but fall well below steady-flow on the downstroke. This overshoot becomes larger as K increases. Its remarkable magnitude is estimated, for example, by comparing the curves of normal force between Figs. 9 & 4. The peak of the graph moves to higher α and at $K=0.04$ exceeds its steady-state value by over 50%. As can be concluded from prior tests and from the flow-visualization analyses in Ref. 26, behavior of this sort is connected with delays in the breakdown or "bursting" of the L.-E. vortex system on the upstroke, followed by a lag in its reestablishment as the α returns toward zero.

The time histories of pitching moment reveal the same increasing trends, and it can be inferred that the center of normal force moves forward on the wing as the chordwise location of vortex breakdown proceeds forward during the upstroke. It is regarded as important for the feasibility of high- α maneuvers that, unlike what has been observed on

pointed bodies of revolution and delta wings in sideslip, rolling moments stay consistently very small. At no time is the center of lift found to move off the wing centerline by more than about 0.5% of the wingspan. These same observations hold for the AR=1.5 model. At AR=1 rolling moments show a more erratic behavior between $\alpha = 25^\circ$ and 55° , especially at very low K. One believes, however, that their excursions are not beyond the ability of aerodynamic controls to balance.

Three additional figures are included as representative of the extensive data collected during this program. In Fig. 10 are plotted the five aerodynamic coefficients for the AR=1.5 model at the high K=0.06. The mild oscillations seen, for instance, in all the curves during downstroke are not regarded as indications of experimental inaccuracy. They are reproducible in repeated tests and are, therefore, in need of explanation. Figure 11 demonstrates the influence of parameter K on normal force for AR=1. The solid curves here are for very slow variation of α ; it is not known whether the small differences between up- and downstroke constitute some sort of hysteresis or merely test imprecision. The final example, Fig. 12, shows the effect on normal force of varying Re between .45 and .85 million for the AR=1.5 wing at K=0.02. As in other experiments that have been conducted on deltas with sharp leading edges over considerably wider ranges of this parameter, it is not felt that any significant influence of Re on resultant airloads can be detected.

Unsteady Effects on Turning

The measurement program reviewed in the preceding section provides, perhaps for the first time, a chance to quantify the potential for enhanced fighter agility inherent in the remarkable flow unsteadiness over pitching delta wings. For many years the favorable and unfavorable effects of "dynamic stall" have been studied for wings of moderate to high AR, rotors, wind turbines, etc. It is foreseen that very detailed analyses of this subject for low-AR aircraft, including trajectory optimizations and combat simulations, will be required before new designs and operational procedures can be adopted. Certainly unsteady wind-tunnel testing of complete models will become routine practice. At the current level of understanding, however, a much simpler approach seems all that is justified.

For the present investigation, it was therefore decided simply to reanalyze the response of the "generic" aircraft of Ref. 7, as it executes turning maneuvers defined according to the time histories of the controls $\alpha(t)$ and $\phi(t)$ taken from Well et al. (7). Based on the

properties of typical fighters discussed in Refs. 3 and Ransom (20), this vehicle has a mass of 10,617 kg and corresponding moments & product of inertia. The double-delta wing of Ref. 7, with S=57.7 m², is replaced by a single sharp-edged delta of AR=2 so as to permit direct use of data like that on Figs. 6-9.

As in Refs. 3, it is assumed that rotational motions can be accomplished so rapidly as to place no constraint on the vehicle dynamics. Accordingly, trajectory computations can be carried out as if it were a point mass *m*. Maneuvers are then described by the time histories of airspeed *V*, flight-path angle Γ above the horizontal, and azimuth angle χ -- measured from a horizontal datum clockwise around to the vertical plane which contains *V*. The state vector *V*, Γ , χ is governed by three nonlinear, first-order differential equations, as follows:

$$m\dot{V} = T \cos \alpha - D - mg \sin \Gamma \quad (4)$$

$$mV\dot{\Gamma} = [T \sin \alpha + L] \cos \phi - mg \cos \Gamma \quad (5)$$

$$(mV \cos \Gamma) \dot{\chi} = [T \sin \alpha + L] \sin \phi \quad (6)$$

There are three auxiliary kinematic relations for rate of change of altitude *h* and two horizontal coordinates *x*, *y* in a (no-wind) earth-fixed triad:

$$\dot{x}_e = V \cos \Gamma \cos \chi \quad (7)$$

$$\dot{y}_e = V \cos \Gamma \sin \chi \quad (8)$$

$$\dot{h} = V \sin \Gamma \quad (9)$$

Equations (7)-(9) can readily be used to construct the trajectory in space, but results of this sort are not given here.

Before presenting some solutions of the system (4)-(6), a few remarks are in order. In Refs. 3 a fourth equation was discussed which connects the rate of decrease of mass *m* to thrust *T* and engine fuel-consumption data. All the maneuvers of interest here occur in such short intervals, however, that *m* is essentially constant. There is a body axis *x* along the zero-lift direction and inclined at angle α above the flight path, but ϕ is bank angle about velocity *V*, positive to depress the right wing below the horizontal. In Refs. 3, *T* and a drag-brake rotation angle are used as auxiliary controls. Along with α and ϕ , the values used for these are taken straight from that source.

Except for the coefficients *C_L* and *C_D*, all information needed for the trajectory calculations can be taken from the large appendix of the DFVLR report, part of Refs. 3 and supplied to the authors by Dr. Well. As a quantitative approach to the primary objective of this paper, a scheme has been devised to make direct comparisons between similar tra-

jectories determined, respectively, from quasi-steady aerodynamic information and corresponding unsteady data. Steady and unsteady coefficients were taken from the same value of α at each value of t called out in a numerical integration of Eqs. (4)-(6). The steady C_L and C_D come from the dotted and dash-dot curves on Fig. 4, respectively. The unsteady data come from curves like those on Figs. 6-9 with the value of K estimated as closely as possible from the prescribed history of the control α . Obviously, the upper branch of the curve is used when α is increasing and the lower when α is decreasing.

Since the lift and drag information employed here does not agree exactly with that in Refs. 3 (cf. Fig. 1 of the paper in J. Guidance, Control and Dyn.), one must ensure that the trajectories calculated from steady data are reasonably close to one another. Comparisons are made in certain of the following examples. The approach used here in order to isolate unsteady effects is believed, however, to be the only logical one.

The maneuvers chosen for study are simple; a very recent article⁽²¹⁾ shows that they do resemble several of those being used for flight demonstration in a program conducted by USAF and NASA. Most cases, as in earlier analytical studies, emphasize a reorientation of the fuselage axis and/or the velocity vector in minimum time from a given initial state. It is generally agreed that these objectives are closely associated with maximum attainable values of the pitching angular velocity $\dot{\alpha}$. This quantity is, therefore, the figure of merit employed here. No attempt is made to meet prescribed final conditions or to optimize, since such sophistication is beyond what can be justified in the light of present approximations. Results of the selected examples are now listed and illustrated, each case being identified with its number from Refs. 3.

(1) 4.2.2-1 -- A horizontal turn, with the objective of rotating the velocity vector through 180° . Initial velocity is 100 m/s, and α is constrained to be less than about 28° . This is clearly not a "supermaneuver" but is used to provide a standard of reference. Figure 13 plots the prescribed angles of attack and bank as spline curve fits to data given for six time instants on page 6 of the Refs. 3 appendix. Figures 14, 15 and 16 show, respectively, the histories of airspeed, angular velocity and normal load factor n_z over the nearly 8 s required for the conventional turn. Note that the curves computed with steady (dotted) & unsteady (solid) airloads agree closely, as anticipated in view of the closeness of the coefficient plots (e.g., Fig. 11) below $\alpha=28^\circ$. (The scales are greatly expanded on Figs. 14-16.) Incidentally, n_z is calculated in conventional fashion, e.g.

from Eqs. (12) of Refs. 3. Convergence studies using progressively lower steps in the time integrations have shown all results to be accurate within the precision of plotting. Similar good agreement was obtained here with the variations of n_z , heading and flight-path angles. It can be concluded that flow unsteadiness does not improve the execution of maneuver 4.2.2-1.

(2) 4.2.6-1 -- A vertically upward turn whose objective is to reverse the axis of the fuselage but with no final constraint on α or flight-path angle. The initial velocity is 100 m/s, again selected because high- α agility is best demonstrated at low speeds, where excessive acceleration can be avoided. The "controls" are plotted in Fig. 17 over the 5.4 s required for the maneuver according to Refs. 3. The wings remain essentially level, and it is remarked that this variation of α seems more realistic than the fluctuating one shown on page 102 of the Refs. 3 appendix. From Fig. 17 and the airspeed history on Fig. 18, it was determined that the best estimates of unsteady airloads should be taken from upward-ramp tests at $K = 0.03$. Given these data, Eqs. (4)-(6) yield the responses graphed on Figs. 18-21. The increased drag at high α produces the small unsteady reduction in V on Fig. 18. Pitch rates on Fig. 19 are seen to be considerably higher with unsteadiness accounted for, especially toward the end of the turn. Since the path angle Γ (Fig. 20) is one possible determinant of when success is achieved, one sees that a value of 90° is reached 0.4 s (or almost 10%) faster than prior estimates would indicate. Figures 18 & 20 contain triangular points taken right from the tables of Refs. 3 and suggest, in this case, that the differences between the airloads used there and here do not lead to large discrepancies. Figure 21, finally, implies that the normal accelerations and the associated structural loads are not affected unfavorably by unsteadiness and, in fact, are somewhat lower near the end of the turn.

(3) 4.2.7-1 -- A vertically upward turn whose objective is to reverse directions of both the fuselage axis and airspeed vector at the top. Again, initial V is 100 m/s and α is unconstrained. It is worth mentioning that no time allowance is made at the end of these two maneuvers for the 180° -roll required for bringing the cockpit upright, as in an Immelmann turn. The assumption is that these adjustments can be made rapidly; they are unlikely to benefit much from unsteady flow. The controls for 4.2.7-1 appear on Fig 22. Figures 23-24 graph corresponding histories of V , $\dot{\alpha}$ and n_z . In this case the $[1 - \cos(\alpha)]$ unsteady data for $K = 0.04$ were found to provide the best approximations. As with 4.2.6-1 unsteady effects reduce the airspeed and yield (here more modest) improvements in

turn rate during the high- α portion of the turn. Load factors (Fig. 25) prove somewhat higher up to about $t = 4$ s, but this is not believed to be an unsteady effect because the α 's are relatively low in this range.

(4) 4.3-2 -- As sketched in Fig. 1, this is a rather violent supermaneuver wherein the aircraft starts and ends at the same point in space but with both the axis and airspeed vector reversed. Initial speed is 100 m/s, and α is unconstrained. In Refs. 3 the estimate is that a 14% time advantage results from turning this way rather than using banks in a horizontal plane under constrained α , even with both maneuvers performed optimally. It is evident from Fig. 1, however, that automatic stabilization and control will be required to hold zero sideslip and otherwise follow this sinuous path.

Figure 26 furnishes curve-fits to the $\alpha(t)$ and $\dot{\phi}(t)$ from Refs. 3. Again the sinusoidal airload data for $K = 0.04$ seemed most suitable for supplying unsteady effects during the high- α transient. Figures 27-29 give the steady-vs.-unsteady comparisons. On the airspeed curves, Fig. 27, the triangles show that present steady results almost coincide with those of Refs. 3, except quite near to the maneuver's end. Figure 28 yields the interesting information that there are substantial unsteady improvements in turn rate through the increasing- α phase but that due to combinations of dynamic effects nothing is lost during the downstroke. Load factors (Fig. 29) show some modest increase during the first sharp pull-up but remain slightly below their steady values for the rest of the turn.

(5) 4.2.7-8 -- A reversing vertically upward turn similar to 4.2.7-1, but with initial velocity 200 m/s and α limited below 70° . Several other of the Refs. 3 maneuvers have been analyzed in a manner similar to the above, and it would be misleading to imply that, in all cases, the influence of unsteadiness will give rise to faster turns with no penalty in terms of structural loads. In general, it is found that examples starting above $V = 100$ m/s are not so favorable. The low-altitude "corner velocity" for the aircraft studied here is around 145 m/s, and one speculates that beyond this airspeed there is little to be gained, because of load-factor limitations.

Figures 30-33 plot the same information for 4.2.7-8 as has been given for the foregoing cases. The sinusoidal airload data for $K = 0.02$ were used in the unsteady calculations. Figure 31 shows that drag overshoot causes some bleeding off of airspeed, but the Fig. 32 turn-rate advantages, which occur only below the "corner," are not impressive. The n-

peak on Fig. 33 is unacceptable, and unsteadiness is seen to increase it by approximately one "g."

A Qualitative Aerodynamic Theory

There is a long history of attempts to extend to time-dependent motions the many steady-flow theories that have been proposed to account for the organized pattern of free vortices that develops above slender, pointed wings as α is increased (Rom⁽¹⁴⁾ summarizes the latter thoroughly). The contributions of Lowson⁽²²⁾, Dore⁽²³⁾ and Randall⁽²⁴⁾ from England in the 1960's deserve first mention. More recently adaptations of panel methods have been published (e.g., Levin & Katz⁽²⁵⁾), and van Niekirk⁽²⁶⁾ modified the leading-edge-singularity scheme of Polhamus⁽²⁷⁾ to account for time-varying α on a delta wing. Two comments are offered regarding all of this work. The first is that, for values of parameters K or k typical of supermaneuvers, the airloads they predict are essentially quasi-steady. Secondly, none seems capable of modelling vortex breakdown. Indeed, the authors believe that a fully rational theory would have to be based on the methods of computational fluid dynamics and would have to account for large volumes of separated, turbulent flow. Analyses of this sort, feasible of extension to α 's as large as 90° , are probably well beyond the scope of even the most powerful current CFD methods.

Granted the impossibility of reliable predictive tools in the near future, one is forced to conclude that unsteady wind-tunnel testing is the only alternative available to the designers of agile aircraft. Every flight vehicle must pass through a preliminary design phase, however, when its configuration is not well enough established to permit model construction. One is perhaps justified, in such a situation, when he puts forth a purely "empirical" or "qualitative" attempt to reproduce the principal features of a phenomenon.

Any such approach must rely, first of all, on estimates of vortex breakdown whose hysteresis is known^{(10),(21)} to be the controlling cause of unsteadiness. At the higher Reynolds nos. breakdown is a rather sudden process. Let it be assumed that information is available from sources like Refs. 16, 18-24 and 26 on a quantity x_b , as it varies with α during prescribed motions (ramp, sinusoid) for a useful range of a parameter like K . x_b is here defined to be the forward limit of an identifiable breakdown region.

As an example of the sort of data needed, Fig. 34 from Jarrah⁽²⁸⁾ gives estimates of the angles where x_b passes the 75%-midspan-chord station of an AR=1 delta on the up- and down-strokes of

sinusoids between $\alpha = 0^\circ$ and 90° . From flow visualizations this quantity proved to depend on K only; for the upstroke, it settles down fairly quickly to values near 45° . Jarrah⁽²²⁾ provides similar data for chordwise stations at 50% and the trailing edge. The results are consistent between sinusoidal and ramp motions, and they are found to agree with-in measurement accuracy with the data of Reynolds and Abtahi⁽²¹⁾ for an almost identical wing model.

In the spirit of Ericsson's imaginative insights (Ref. 37 contains recent examples), let it be assumed that the distribution of aerodynamic force per unit chordwise distance is made up of three parts: (1) A portion determined from the rate of change of crossflow momentum, in a manner resembling the low-AR theory of Jones⁽²³⁾ but with the slabs of fluid taken normal to the wing surface at α . (2) A portion calculated on a quasi-steady basis by rotating the L.-E. suction force through 90° , as proposed by Polhamus⁽²⁴⁾. At higher α 's, loads (1) & (2) act only ahead of $x_0(\alpha(t))$. (3). A portion, dominant at the higher α 's and calculated from the Betz⁽²⁵⁾ crossflow-drag model. This turns out nearly proportional to $C_{D0}\sin^2\alpha$. C_{D0} itself is chosen empirically from the drag at $\alpha=90^\circ$ measured for a given K.

For pitching $\alpha(t)$ about a fixed axis at two-thirds midspan chord, formulas for normal force and moment about that same axis are given in Eqs. (10) & (11), which follow. The moment can be transferred to 77%-chord in the usual way for experimental comparisons. It seems consistent to assume that the force resultant acts perpendicular to the wing, so that lift and drag are just the $\cos\alpha$ and $\sin\alpha$ components of C_N . In these formulas the three portions listed above are contained sequentially in the three braces. "sin" & "cos" are abbreviated "s" & "c."

$$C_N = (\pi/6)(x_B/c_0)^2 \text{ctn}\eta(6s2\alpha - 8(\dot{c}_0/V)\alpha + 16(\dot{c}_0/V)(x_B/c_0)\alpha + (\dot{c}_0^2/V^2)[3(x_B/c_0)^2 - (8x_B/3c_0)]) + (\pi/6s\eta)(x_B/c_0)^2(6s^2\alpha + 8(\dot{c}_0/V)[(x_B/c_0) - 1]s\alpha + (\dot{c}_0/V)^2[3(x_B/c_0)^2 + (8/3) - (16x_B/3c_0)]) + C_{D0}(s^2\alpha + (1/18)(\dot{c}_0/V)^2) \quad (10)$$

$$C_{M0} = -2\pi(x_B/c_0)^2(c_0/E)\text{ctn}\eta[(x_B/c_0) - 1]s2\alpha + (\dot{c}_0/V)[3(x_B/c_0)^2 - 4(x_B/c_0) + 4/3]\alpha + (\dot{c}_0^2/V^2)[(3/5)(x_B/c_0)^2 - (x_B/c_0)^2 + (4x_B/9c_0)] - (\pi/6s\eta)(x_B/c_0)^2(c_0/2) * (4[(x_B/c_0) - 1]s^2\alpha + (\dot{c}_0/V)[3(x_B/c_0)^2 - (16x_B/3c_0) + (8/3)]s\alpha + (\dot{c}_0/V)^2[-(16/9) + (16x_B/3c_0) - 4(x_B/c_0)^2 + (12/5)(x_B/c_0)]) - C_{D0}(c_0/E)((1/9)(\dot{c}_0/V)s\alpha - (1/135)(\dot{c}_0/V)^2) \quad (11)$$

For the delta wing of AR=1, Figs. 35 and 36 show as solid curves the predictions of Eqs. (10) & (11), plotted vs. α for K=0.06. The moments of Fig. 36 are about the 77%-chord axis, so that a direct comparison is possible with the

measured data, plotted as dash-dots. This aspect ratio was selected because spline fits could be used for x_B estimates drawn from Reynolds & Abtahi⁽²¹⁾ and the Ref. 26 flow visualizations. All that can be stated is that this first attempt at a "theory" reproduces the qualitative behavior of the airloads. Similar calculations for AR's 1.5 and 2 yield comparable or better accuracy. It also appears possible, by more realistic handling of the parameter x_B , to get better agreement over the high- α portions of these curves. Finally, resort to more precise theories like that of Dore⁽²⁶⁾ is likely to give improvements in the α -range where breakdown has little influence on the loading.

Concluding Remarks

A program has been reviewed of airload measurements on a family of low-AR delta wings with sharp leading edges, subjected in the wind tunnel to large-amplitude pitch transients involving α 's going as high as 90° . Rather small values of the pitch-rate parameter K were used, representative of maneuvers anticipated for "agile" aircraft. Even for these modestly unsteady motions, it is found that force and moment overshoots can exceed by 50% their steady-state counterparts. The explanation lies in the hysteretic behavior of the breakdown location of L.-E. vortices.

By means of examples based on low-speed, high- α maneuvers from the literature, an attempt is made to demonstrate that considerably higher turn rates can be achieved than would be predicted from steady-state airload data. This enhanced maneuverability is, by no means, always accompanied by a penalty in terms of load factor and associated pilot discomfort or structural overstress. Not all the cases studied show these advantages, however, because the improved agility appears to exist only at flight speeds well below the "corner velocity." It is believed that designers of these vehicles (and their control systems) should certainly seek to take account of the potentialities of flow unsteadiness.

The paper concludes by proposing a very approximate theoretical model which tries to include the breakdown hysteresis as part of a three-term representation of the unsteady chordwise load distribution. The resulting estimates for normal force and moment due to pitching motion exhibit the same features found in test data, but more refinement will obviously be needed before this model has any chance of quantitative success. It is put forth in the conviction that a wholly rational theory must await extensive developments in the field of CFD. Lacking such tools, however, one concludes that wind-tunnel tests on pitching models of agile-aircraft designs will furnish the only pre-flight source of the information required to analyze their maneuvers.

Acknowledgements

This investigation was supported by National Aeronautics & Space Administration under Grant NCA2-287, part of the Joint Research Interchange program with Ames Research Center, as well as by the United States Air Force Office of Scientific Research under Contract AFOSR 84-0099. The authors are appreciative of the important assistance given by Mr. Richard J. Margason, Chief, Low Speed Aerodynamics Branch of NASA Ames. Ms. Joyce Parker prepared this manuscript.

References

1. Herbst, W. B., "Future Fighter Technologies," Journal of Aircraft, Vol. 17, No. 8, August 1980, pp. 561-566.
2. Herbst, W. B., "Dynamics of Air Combat," Journal of Aircraft, Vol. 20, 1983, pp. 594-598.
3. Well, K. H., Faber, B., and Berger, E., "Optimization of Tactical Aircraft Maneuvers Utilizing High Angles of Attack," Journal of Guidance, Control and Dynamics, Vol. 5, 1982, pp. 131-137. (See also "Optimale taktische Flugmanöver für ein Kampfflugzeug der 90er Jahre," Interner Bericht A-532-79/6, 1979, DFVLR, Federal Republic of Germany.)
4. Dietz, W. C., and Duc, J.-M., Eds., "Combat Aircraft Maneuverability," AGARD Conference Proceedings No. 319, 1981, NATO Advisory Group for Aerospace Research and Development.
5. Many authors, Supermaneuverability Technical Specialists Meeting, 1984, USAF Wright Aeronautical Laboratories, Wright-Patterson AFB, Ohio.
6. Anderson, J., "Agile Fighter Aircraft Simulation," AIAA 89-0015, presented at 27th Aerospace Sciences Meeting, Reno, January 1989.
7. Ashley, H., "On the Feasibility of Low-speed Aircraft Maneuvers Involving Extreme Angles of Attack," Journal of Fluids and Structures, Vol. 1, No. 3, 1987, pp. 319-335.
8. Lang, J. D., and Francis, M. S., "Unsteady Aerodynamics and Dynamic Aircraft Maneuverability," AGARD Conference Proceedings No. 386, 1985, pp. 29-1-29-19, NATO Advisory Group for Aerospace Research and Development.
9. Naumowicz, T., Jarrah, M. A., and Margason, R., "Aerodynamic Investigation of Delta Wings with Large Pitch Amplitude," AIAA 88-4332-CP, presented at Atmospheric Flight Mechanics Conference, Minneapolis, August 1988.
10. Jarrah, M. A., "Low-speed Wind-tunnel Investigation of the Flow about Delta Wings Oscillating in Pitch to Very High Angle of Attack," AIAA 89-0293, presented at 27th Aerospace Sciences Meeting, Reno, January 1989.
11. Many Authors, "Dynamic Stability Parameters," AGARD Conference Proceedings No. 235, 1978, NATO Advisory Group for Aerospace Research and Development.
12. Parker, A. G., "Aerodynamic Characteristics of Slender Wings with Sharp Leading Edges—a Review," Journal of Aircraft, Vol. 13, 1976, pp. 161-168.
13. Wendt, J. F., Ed., "High Angle-of-Attack Aerodynamics," AGARD Lecture Series No. 121, 1982, NATO Advisory Group for Aerospace Research and Development.
14. Rom, J., "Current Problems and Methods in High Angle of Attack Aerodynamics," Course Notes, Stanford Univ., Stanford, CA (to be published as book).
15. Lowson, M. V., "Visualization Measurements of Vortex Flows," AIAA 89-0191, presented at 27th Aerospace Sciences Meeting, Reno, January 1989.
16. Thompson, S., Batill, S., and Nelson, R., "The Separated Flow Field on a Slender Delta Wing Undergoing Transient Pitching Motions," AIAA 89-0194, presented at 27th Aerospace Sciences Meeting, Reno, January 1989.
17. Lowson, M. V., "Some Experiments with Vortex Breakdown," Journal of the Royal Aeronautical Society, Vol. 68, 1964.
18. LeMay, S. P., Batill, S., and Nelson, R., "Leading Edge Vortex Dynamics on a Pitching Delta Wing," AIAA Paper 88-2559-CP, June 1988.
19. Gad-el-Hak, M., and Ho, C. M., "The Pitching Delta Wing," AIAA Journal, Vol. 23, No. 11, November 1985, pp. 1660-1665.
20. Gad-el-Hak, M., and Ho, C. M., "Unsteady Vortical Flow Around Three-Dimensional Lifting Surfaces," AIAA Journal, Vol. 24, No. 5, May 1986, pp. 713-721.
21. Reynolds, G. A., and Abtahi, A. A., "Instabilities in Leading-Edge Vortex Development," AIAA 87-2424, presented at Applied Aerodynamics and Atmospheric Flight Mechanics Conference, Monterey, August 1987.
22. Atta, R., and Rockwell, D., "Hysteresis of Vortex Development and Breakdown on an Oscillating Delta Wing," AIAA Journal, Vol. 25, 1987, pp. 1512-1513.
23. Wolffelt, K. W., "Investigation on the Movement of Vortex Burst Position with Dynamically Changing Angle of Attack for a Schematic Deltawing in a Water-tunnel with Correlation to Similar Studies in Windtunnel," AGARD Conference Proceedings No. 413, 1986, pp. 27-1 - 27-8, NATO Advisory Group for Aerospace Research and Development.
24. Soltani, M. R., Bragg, M. B., and Brandon, J. M., "Experimental Measurements on an Oscillating 70-Degree Delta Wing in Subsonic Flow," AIAA 88-2576-CP, June 1988.
25. den Boer, R. G., and Cunningham, A. M., "A Wind-Tunnel Investigation at Low Speed about a Straked Delta Wing, Oscillating in Pitch," AIAA 87-2493, presented at Applied Aerodynamics and Atmospheric Flight Mechanics Conference, Monterey, August 1987.

26. Jarrah, M.-A. M., "Unsteady Aerodynamics of Delta Wings Performing Maneuvers to High Angle of Attack," PhD Thesis, Dept. of Aeronautics and Astronautics, Stanford University, Dec. 1988.
27. Lawford, J. B., and Beauchamp, "Low-Speed Wind-Tunnel Measurements on a Thin Sharp-Edged Delta Wing with 70-deg. Leading-Edge Sweep," British A. R. C. R. & M. 3338, November 1961.
28. Bartlett, G. E., and Vidal, R. J., "Experimental Investigation of Influence of Edge Shape on the Aerodynamic Characteristics of Low Aspect Ratio Wings at Low Speeds," Journal of the Aeronautical Sciences, Vol. 22, No. 8, August, 1955, pp. 517-533.
29. Polhamus, E. C., "Predictions of Vortex-Lift Characteristics by a Leading-Edge Suction Analogy," Journal of Aircraft, Vol. 8, No. 4, April 1971, pp. 193-199.
30. Ransom, S., "Configuration Development of a Research Aircraft with Post-stall Maneuverability," Journal of Aircraft, Vol. 20, 1983, pp. 599-605.
31. Scott, W. B., "Air Force, NASA Conduct Tests to Define Fighter Agility," Aviation Week & Space Technology, Vol. 130, No. 2, January 9, 1989, pp. 45-47.
32. Lawson, M. V., "The Separated Flows on Slender Wings in Unsteady Motion," British A. R. C. R. & M. 3448, 1967.
33. Dore, B. D., "Non-linear Theory for Slender Wings in Sudden Plunging Motion," The Aeronautical Quarterly, Vol. XVII, 1966, pp. 187-200.
34. Randall, D. G., "Oscillating Slender Wings with Leading-Edge Separation," The Aeronautical Quarterly, Vol. XVII, 1966, pp. 311-331.
35. Levin, D., and Katz, J., "Vortex-Lattice Method for the Calculation of the Nonsteady Separated Flow over Delta Wings," Journal of Aircraft, Vol. 18, 1981, pp. 1032-1037.
36. van Niskerk, B., "A Rational Approach to Lifting Surface Theory with Application to High Angles of Attack," SUDAAR No. 555, Department of Aeronautics and Astronautics, Stanford University, June 1986.
37. Ericsson, L. E., "Missile Dynamics Including High Alpha Maneuvers," AIAA 89-0330, Presented at 27th Aerospace Sciences Meeting, Reno, January 1989.
38. Jones, R. T., "Properties of Low-Aspect-Ratio Pointed Wings at Speeds Below and Above the Speed of Sound," NACA Report 835, 1946.
39. Betz, A., "Applied Airfoil Theory," Division J, Vol. IV, Aerodynamic Theory, W. F. Durand, Ed., Dover Publications, New York, 1963, pp. 69-70.

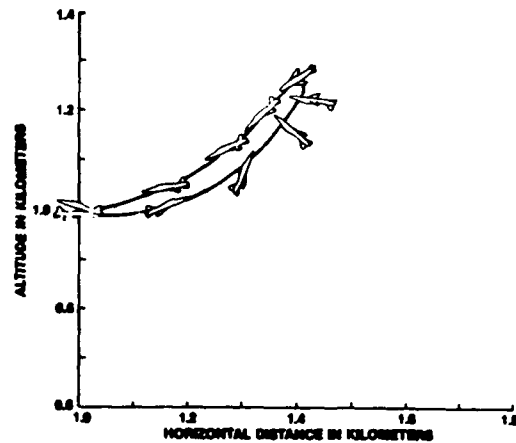


Fig. 1. Vehicle orientations and trajectory in vertical plane for supermaneuver involving reversal of velocity and fuselage axis. Initial and final positions are at the same point in space.

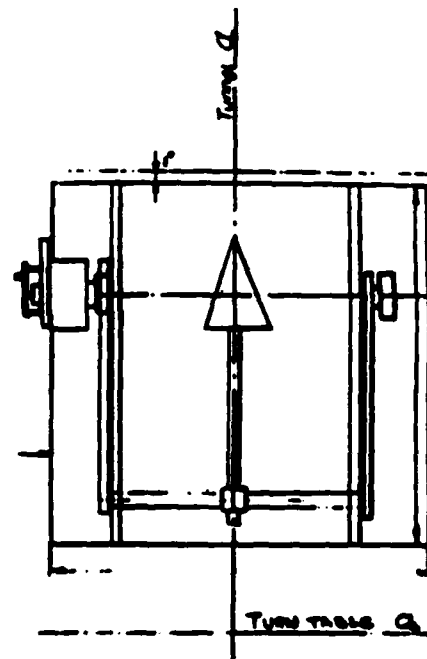


Fig. 2. Downstream view of model, fairings and apparatus for pitch actuation in the wind tunnel.

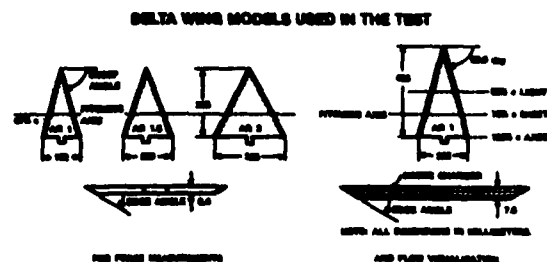


Fig. 3. Models used for airload tests and flow visualization.

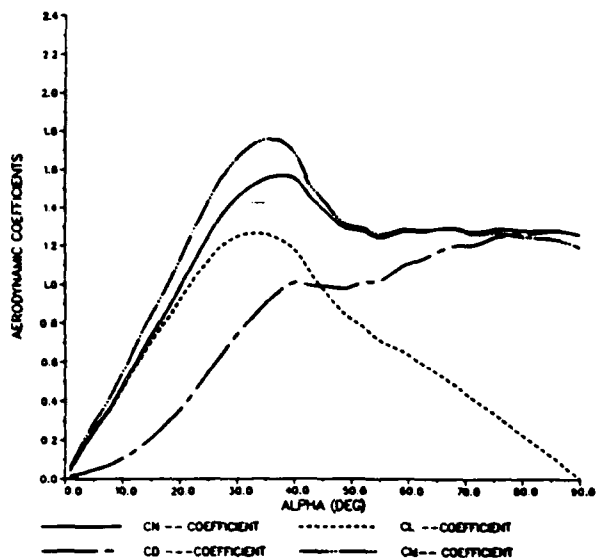


Fig. 4. Plot of four coefficients vs. α for steady flow past delta model of $AR=2$; Reynolds no. $Re = 5.9 \times 10^5$.

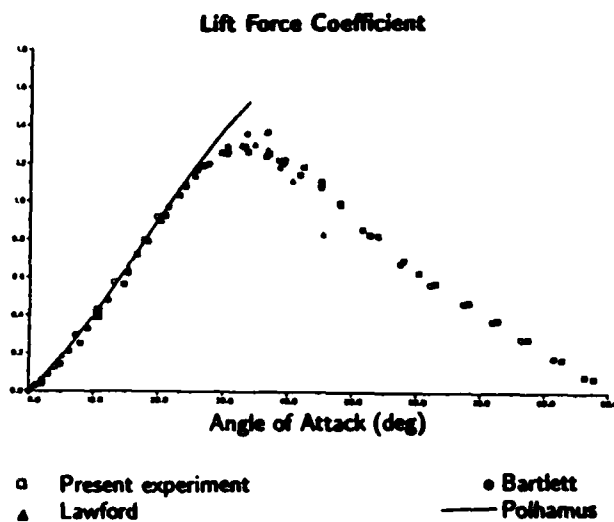


Fig. 5. Steady lift coefficients of $AR=2$ delta model, compared with theory of Polhamus (—) and tests of Lawford (▲) & Bartlett (●).

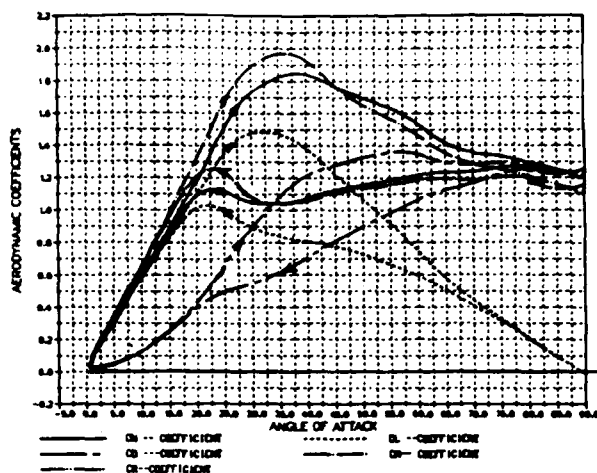


Fig. 6. Coefficients of normal force, drag, rolling moment (essentially zero), lift and pitching moment about 77%-chord axis; these are plotted vs. α for $AR=2$ delta performing the $[1 - \cos \omega t]$ pitch maneuver. Unsteadiness parameter is $K=0.01$, and $Re = 4.5 \times 10^5$.

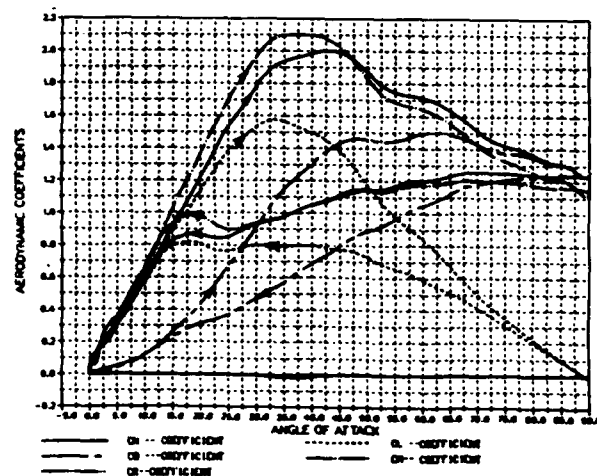


Fig. 7. Same as Fig. 6 for $K=0.02$ and $Re = 6.4 \times 10^5$.

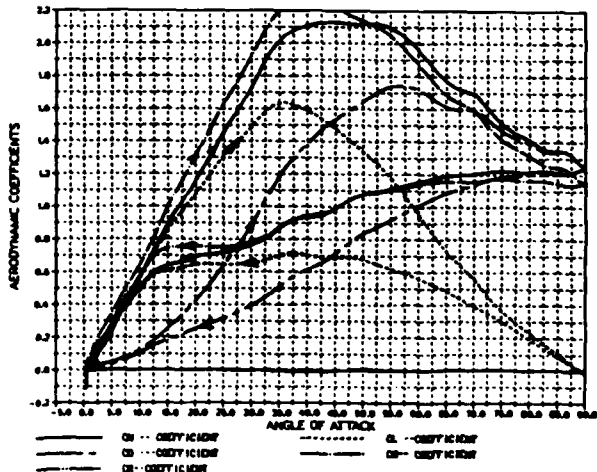


Fig. 8. Same as Fig. 6 for $K=0.03$ and $Re = 4.5 \times 10^5$.

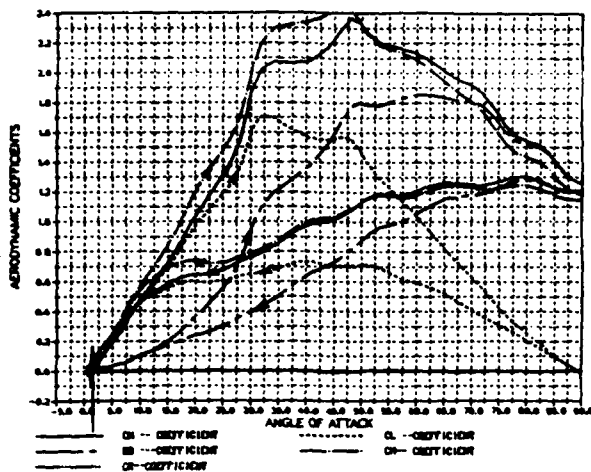


Fig. 9. Same as Fig. 6 for $K=0.04$ and $Re = 4.5 \times 10^6$.

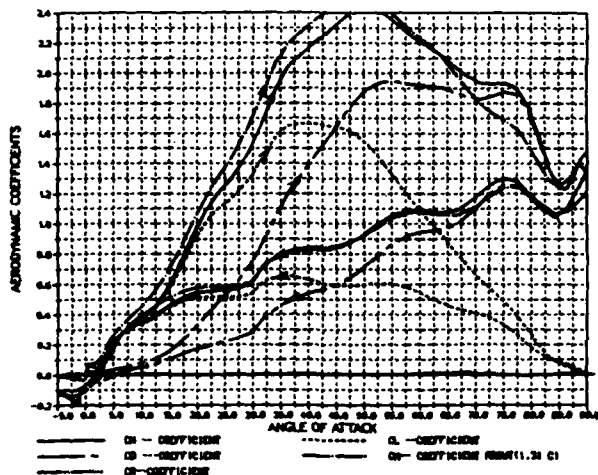


Fig. 10. Same as Fig. 6 for $AR=1.5$ delta at the high value $K=0.06$.

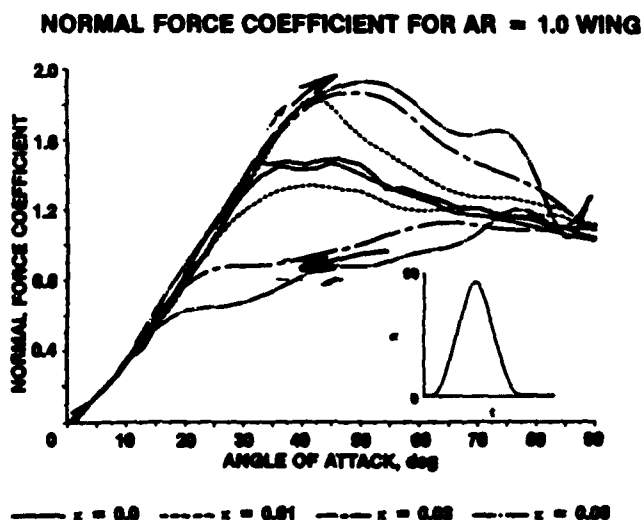


Fig. 11. Normal force C_N vs. α for $AR=1$ delta performing the $[1 - \cos \Omega t]$ pitch maneuver at four values of K .

REYNOLDS NUMBER EFFECTS ($AR = 1.5$ WING, $\alpha = 0.02$)

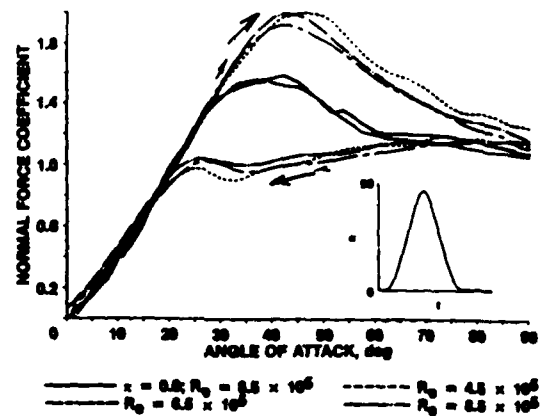


Fig. 12. Effect of Reynolds no. on normal force history for $AR=1.5$ delta at $K = 0.02$.

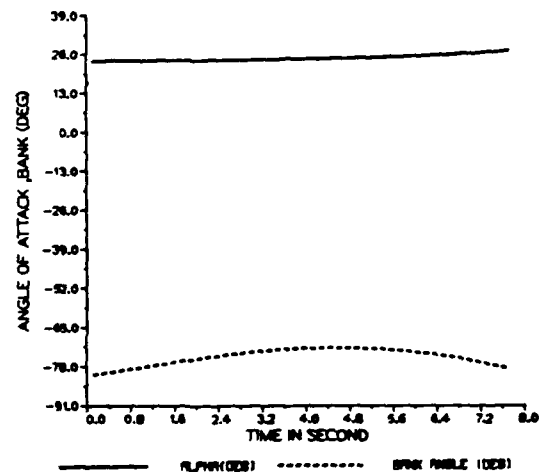


Fig. 13. Time histories of α and β as "controls" for minimum-time conventional turn (No. 4.2.2-1 of Refs. 3).

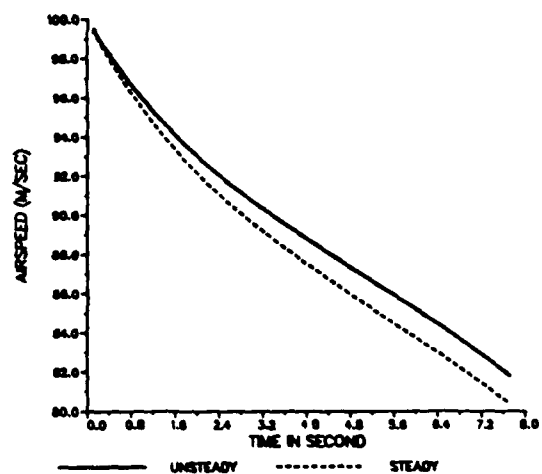


Fig. 14. Histories of airspeed V , calculated for Maneuver 4.2.2-1 with steady (dashed) and unsteady (solid line) airloads.

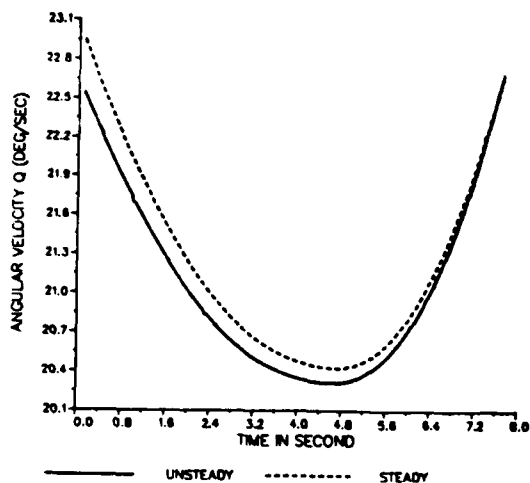


Fig. 15. Histories of pitch rate Q for Maneuver 4.2.2-1.

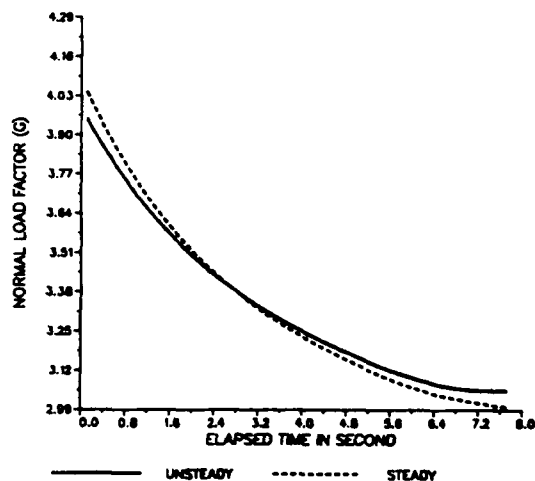


Fig. 16. Histories of normal load factor n_z for Maneuver 4.2.2-1.

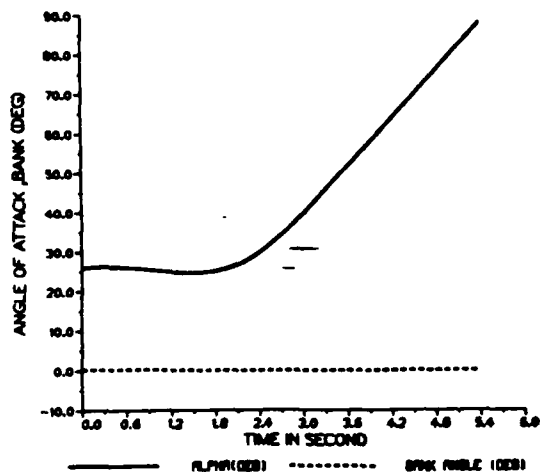


Fig. 17. Time histories of α and ϕ as "controls" for minimum-time vertically-upward turn without α -constraint (No. 4.2.6-1 of Refs. 3).

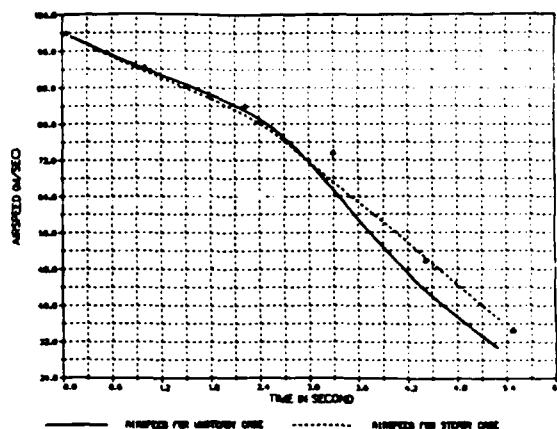


Fig. 18. Histories of airspeed V , calculated for Maneuver 4.2.6-1 with steady (dashed) and unsteady (solid line) airloads. Triangles are points found with aerodynamic data from Refs. 3.

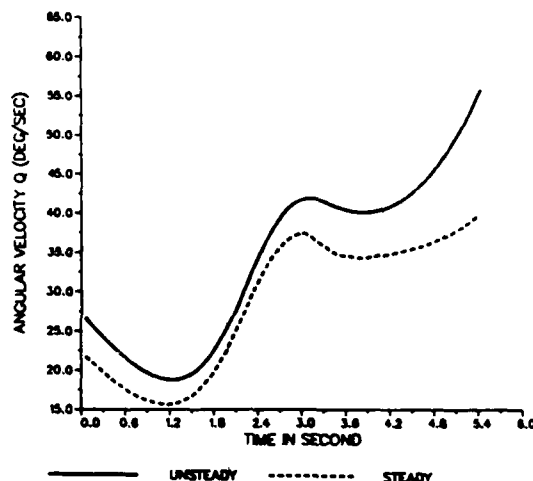


Fig. 19. Histories of pitch rate Q for Maneuver 4.2.6-1.

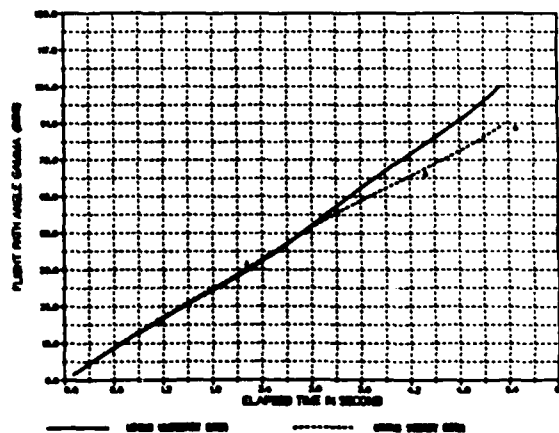


Fig. 20. Histories of flight-path angle γ for Maneuver 4.2.6-1. Triangles are points found with data from Refs. 3.

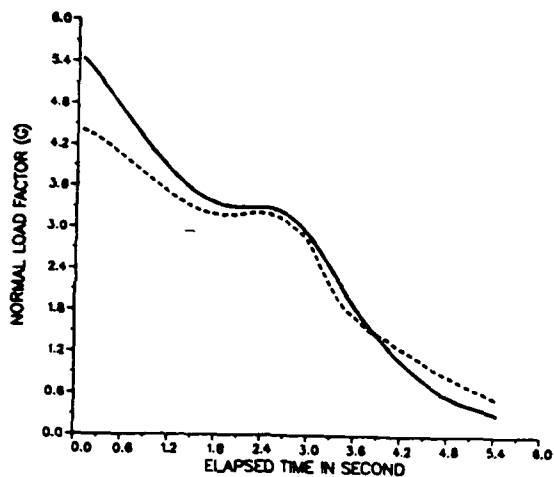


Fig. 21. Histories of normal load factor n_z for Maneuver 4.2.6-1.

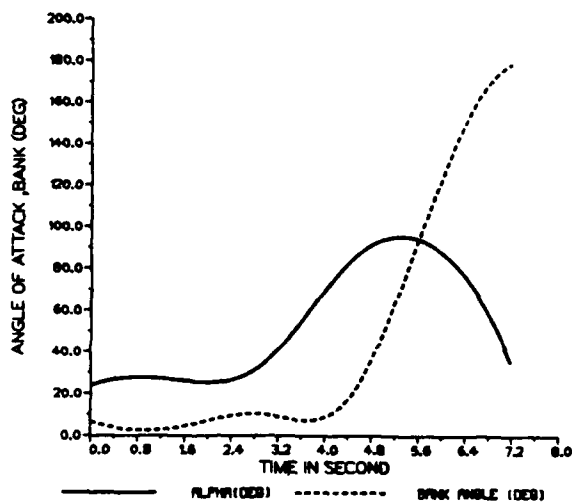


Fig. 22. Time histories of α and ϕ as "controls" for minimum-time vertically-upward turn without α -constraint but with reversal of velocity and fuselage axis (No. 4,2.7-1 of Refs. 3).

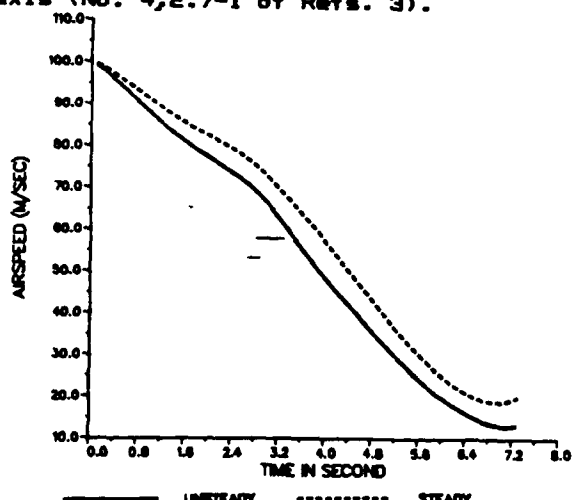


Fig. 23. Histories of airspeed V , calculated for Maneuver 4.2.7-1 with steady (dashed) and unsteady (solid line) airloads.

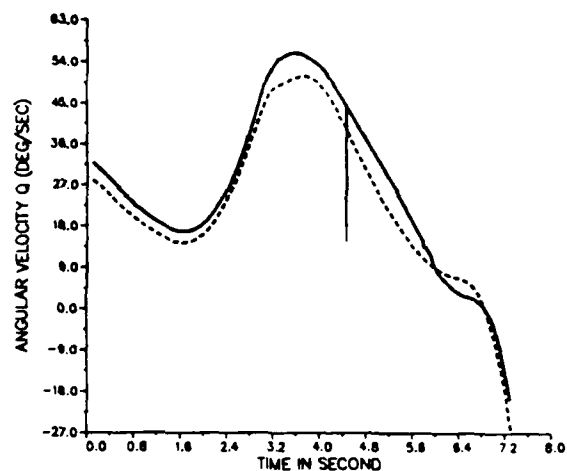


Fig. 24. Histories of pitch rate Q for Maneuver 4.2.7-1.

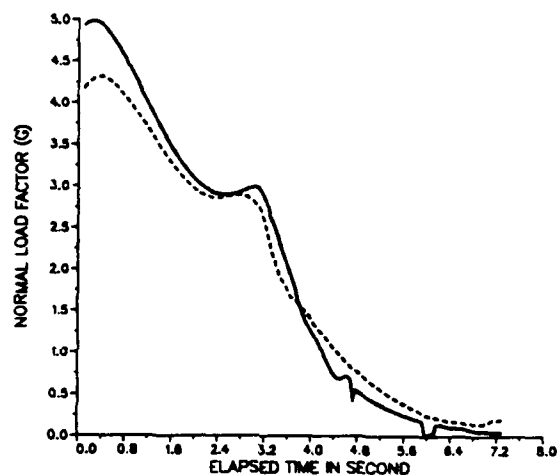


Fig. 25. Histories of normal load factor n_z for Maneuver 4.2.7-1.

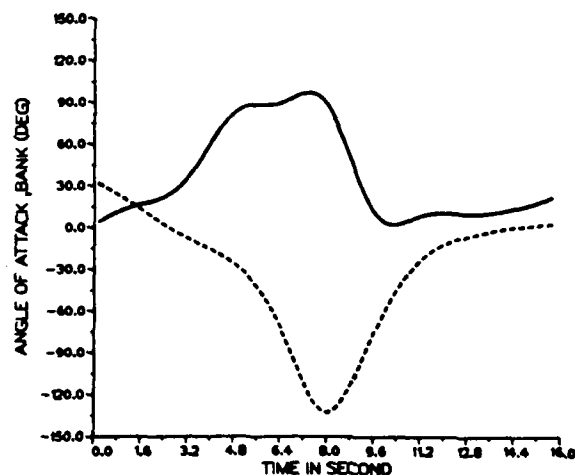


Fig. 26. Time histories of α and ϕ as "controls" for minimum-time reversal without α -constraint (Fig. 1 and No. 4.3-2 of Refs. 3).

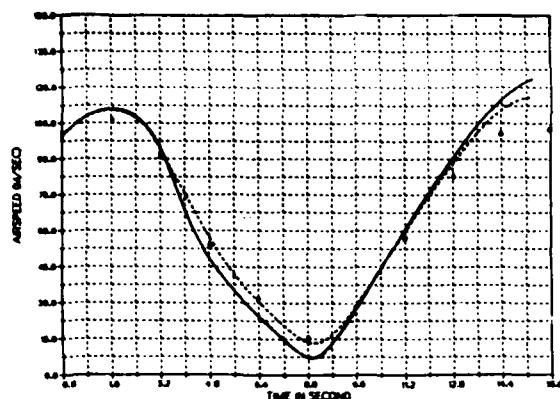


Fig. 27. Histories of air-speed V for Maneuver 4.3-2. Triangles found with data from Refs. 3.

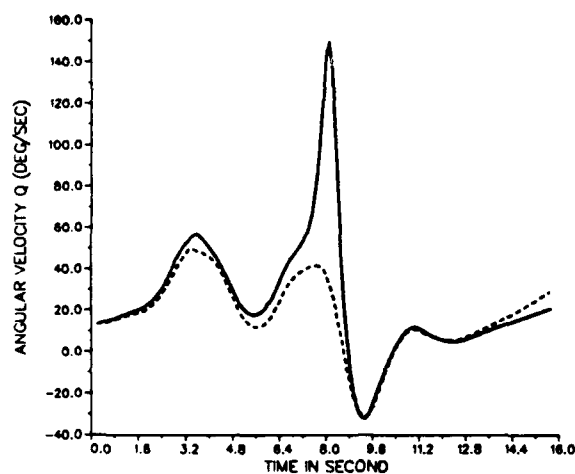


Fig. 28. Histories of pitch rate Q for Maneuver 4.3-2.

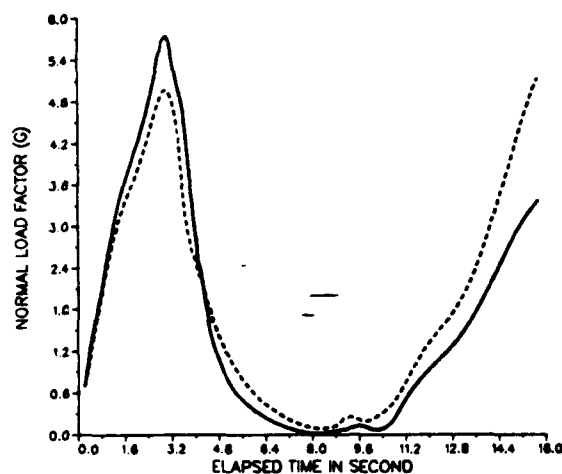


Fig. 29. Histories of normal load factor n_x for Maneuver 4.3-2.

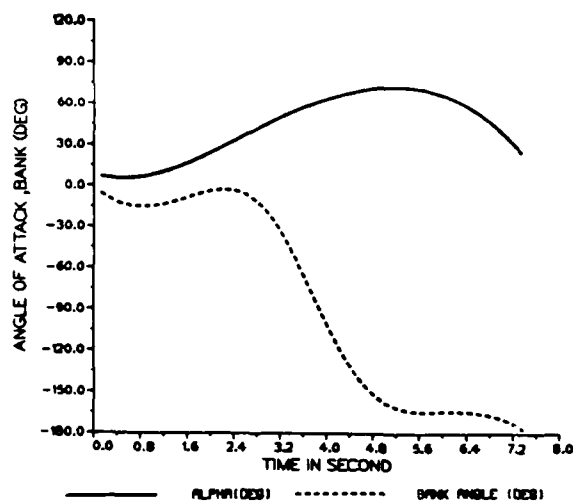


Fig. 30. Time histories of α and ϕ as "controls" for climbing turn similar to Maneuver 4.2.7-1 but with initial speed 200 m/s (No. 4.2.7-8 of Refs. 3).

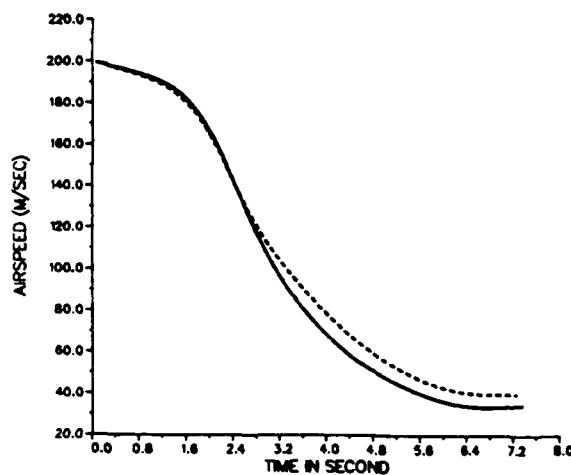


Fig. 31. Histories of airspeed V for Maneuver 4.2.7-8.

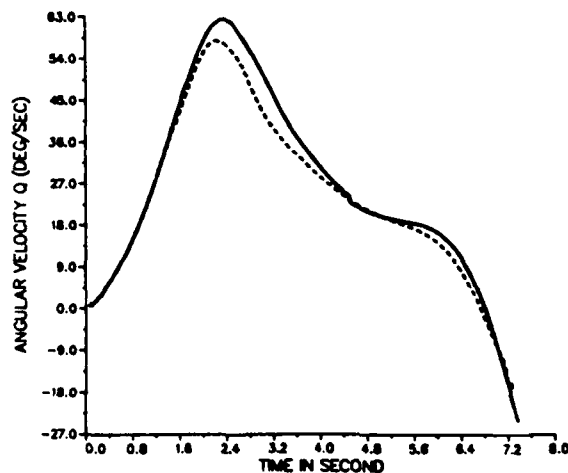


Fig. 32. Histories of pitch rate Q for Maneuver 4.2.7-8.

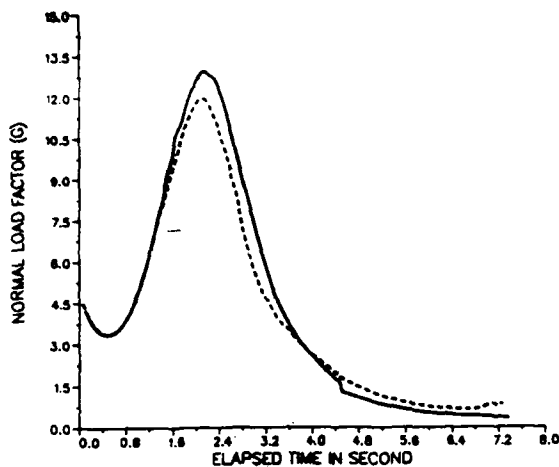


Fig. 33. Histories of normal load factor n_z for Maneuver 4.2.7-8.

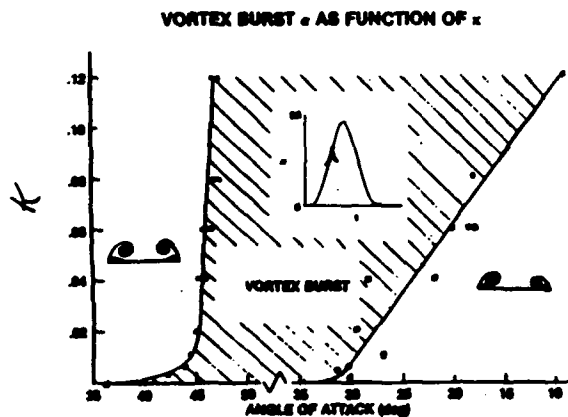


Fig. 34. Angle of attack α at which vortex breakdown passes the 75%-midspan-chord station on AR=1 delta, plotted as a function of parameter K . Left-hand curve is for upstroke and right-hand curve is for downstroke in $[1 - \cos\Omega t]$ pitching.

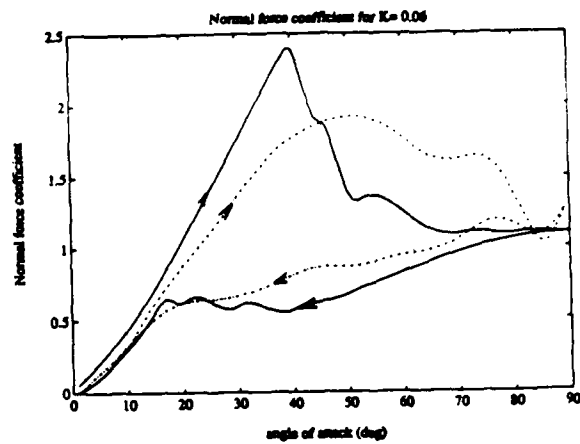


Fig. 35. Normal force plotted vs. α for a $[1 - \cos\Omega t]$ pitch motion by an AR=1 delta model. Prediction of Eq. (10) is compared with measured data (dash-dot curve) for $K=0.06$.

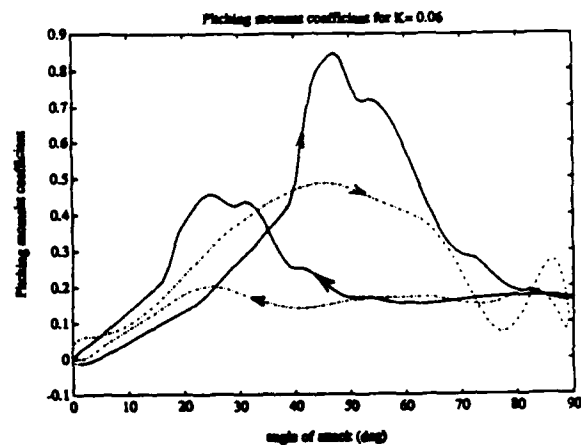


Fig. 36. Pitching moment about 77%-chord axis. Case is the same as Fig. 35, solid line being the prediction of Eq. (11).